International Journal of Chemical, Materials and Biomolecular Sciences
ISSN: 2415-6620
Vol:5, No:2, 2011

Effect of CW Laser Annealing on Silicon Surface for Application of Power Device

Satoru Kaneko, Takeshi Ito, Kensuke Akiyama, Manabu Yasui, Chihiro Kato, Satomi Tanaka, Yasuo Hirabayashi, Takeshi Ozawa, Akira Matsuno, Takashi Nire, Hiroshi Funakubo and Mamoru Yoshimoto

Abstract—As application of re-activation of backside on power device Insulated Gate Bipolar Transistor (IGBT), laser annealing was employed to irradiate amorphous silicon substrate, and resistivities were measured using four point probe measurement. For annealing the amorphous silicon two lasers were used at wavelength of visible green (532 nm) together with Infrared (793 nm). While the green laser efficiently increased temperature at top surface the Infrared laser reached more deep inside and was effective for melting the top surface. A finite element method was employed to evaluate time dependent thermal distribution in silicon substrate.

Keywords—laser, annealing, silicon, recrystallization, thermal distribution, resistivity, finite element method, absorption, melting point, latent heat of fusion.

I. Introduction

POWER Device is the basis of power electronic technology in rapid development with an environmental problem. A power device IGBTs (Insulated gate bipolar transistor) are one of key components of an inverter for hybrid vehicles, and used as a switching device. One characteristic factor is IGBTs consisting of p-type collector on the backside to induce holes during on state to decrease on resistance of the device, as shown in Figure 1. As down sizing the device, it is required to re-activate the backside of IGBT after implanting boron atoms to fabricate p-type layer.

In this study, two laser were employed as backside-activation technique of power device IGBTs by both visible green and Infrared lasers. The two wavelength lasers irradiated the surface of amorphous silicon with the high scan speed of 300 m/min. A finite element method was employed to estimate the surface temperature irradiated by the two lasers with high scanning speed.

II. Experimental

Amorphous silicon substrate was prepared by ion implantation method; Boron was implanted into 3 inches Si(001) substrate with a dose of 5×10^{15} /cm^2 at energy of 60 keV. P ion was also implanted at energy of 60 keV with heavy dose of 1×10^{16} /cm^2. The average depth of implanted ions was estimated to be ∼250 nm by a simulation method using the Stopping and Range of Ions in Matter (SRIM) [1], [2]. The SRIM calculates the stopping and range of ions into matter using a quantum mechanical treatment of ion-atom collisions.

S. Kaneko is with Kanagawa Industrial Technology Center, Kanagawa Prefectural Government, Ebina, Kanagawa, 243-0435 JAPAN (e-mail: satoru@kanagawa-iri.go.jp).

T. Ito, K. Akiyama, M. Yasui, C. Kato, S. Tanaka, Y. Hirabayashi and T. Ozawa are with Kanagawa Industrial Technology Center, Kanagawa Prefectural Government, Ebina, Kanagawa, 254-0435 JAPAN

A. Matsuno and T. Nire are with Phoeton Corp., Atsugi, Kanagawa 243-0021 JAPAN

H. Funakubo and M. Yoshimoto are with Department of Innovative and Engineered Materials, Tokyo Institute of Technology, Yokohama, Kanagawa 226-8502 JAPAN

Manuscript received ; .

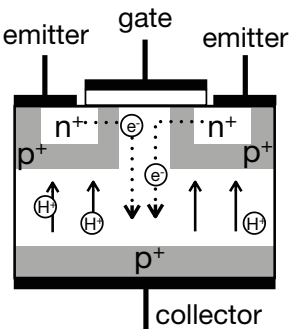

Fig. 1. Schematic of Insulated Gate Bipolar Transistor (IGBT). Re-activation is required on the backside of IGBT.

Two lasers employed to irradiate the amorphous Si substrate were A 532 nm CW laser with a spot size of 10 × 15 μm and laser power ranging from 12 to 18 W, which produced the energy fluency of 24 ∼ 36 J/cm^2. A CW near infrared (NIR) laser also simultaneously irradiated at an energy fluency of 32 J/cm^2 with a wavelength of 797 nm. The two wavelength lasers scanned on the Si substrate with the speed between 300 and 900 m/min. The resistivity was measured by using four point probe method and a finite element method was employed to estimate the surface temperature with time dependency.

III. Results and Discussion

After laser irradiation on the amorphous Si substrate, resistivity was measured by using four point probe. Table I

TABLE I
Sheet resistance after laser annealing. Sheet resistance shows asymmetry along and cross the trace of laser scanning.

scan speed (m/min)	green laser (W)	NIR laser (W)	resistivity // (Ω/□)	resistivity ⊥ (Ω/□)
300	18	100	72	65
300	18	200	64	50
300	18	300	65	50

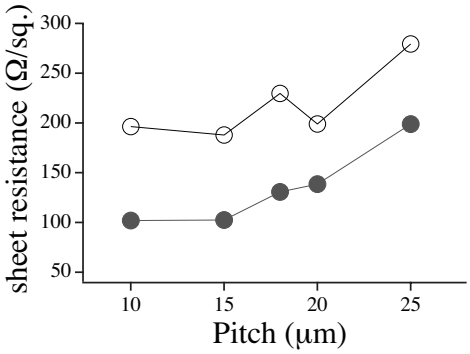

Fig. 2. one example of mesh model consisting two boxes with different mesh size.

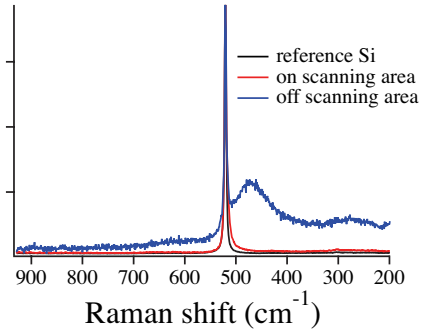

Fig. 3. Raman spectroscopy on laser irradiated area (on scan area) and non irradiated area (off scan area) together with Si substrate as a reference.

shows resistivities of Boron implanted samples. The resistivity was measured along parallel and vertical to laser scanning direction. Interestingly asymmetric resistivities were obtained on almost all samples irradiated in variety of conditions.

Another example of asymmetric resistivity was obtained on samples irradiated with the scanning speed of 900 m/min. Independent on scanning pitch, higher resistivity was obtained across the trace of laser scanning, as shown in figure 2. After optimizing irradiation conditions, scanning speed of 300 m/min. with the assist of the NIR laser prevented these asymmetric resistivity.

Re-crystallization was verified by Raman spectroscopy. Figure 3 shows raman spectroscopy on laser irradiated area (on scan area, red solid line) and non irradiated area (off scan area, blue solid line) together with Si substrate as a reference. A sharp peak from crystal Si was observed at 520 cm^{-1} along the trace of laser scanning (red solid line) while off scan area shows typical broad peak from amorphous Si. The energy fluency of green laser varied from 12 to 18 W. Independent on energy fluency of green laser, raman spectra indicated re-crystallization after the laser scanning. Whether amorphous silicon melt to re-crystallize on laser scanning? A finite element method was employed to estimate surface temperature.

Three dimensional thermal simulation was performed on the Si substrate using the freeFEM3D, which stands for *FREE Finite Element Method in 3 Dimensions*. The freeFEM3D

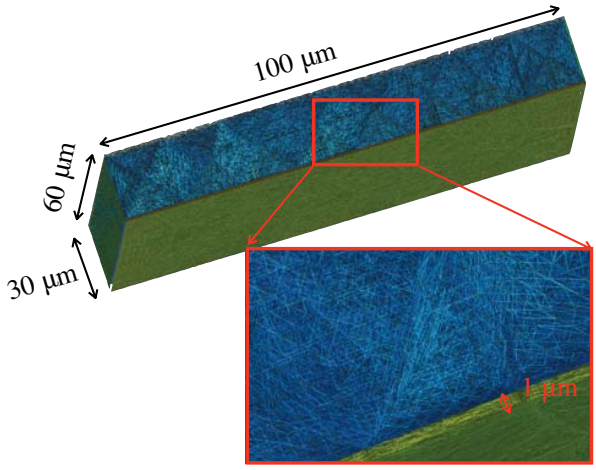

Fig. 4. one example of mesh model consisting two boxes with different mesh size.

solves problem modeled by Partial Differential Equations, so called PDE solver, and is distributed by the General Public License (GPL guidelines). The source code can be found at web site [URL:www.freefem.org/ff3d]. A 64 bit version of freeFEM3D was compiled on Intel Xeon processors with 2.8 GHz on an Apple MacPro.

Si wafer of 100 (length) $\times$ 60 (width) $\times$ 30 (depth) μm was first divided into two boxes, and they were meshed by rough size (a few μm) and by fine size of $\sim$ 50 nm, as sown in Figure 4. The laser irradiated on the fine meshed box and the 3D FEM simulation was applied to the two meshed boxes, and then an optimal condition for interval time δt was determined to be 0.0125 μsec. 3200 steps were required to scan over Si wafer with scan speed of 300 m/min.

The PDE solver, FreeFEM3D, solves the following heat transport equation,

$$\rho\, c_{\rm p}(T)\,\frac{\partial T}{\partial t} - \nabla\,(k(T)\nabla T) = Q(t), \qquad (1)$$

where T is the absolute temperature. $c_p(T)$ and $k(T)$ are temperature dependent variables of the specific heat capacity and the thermal conductivity, respectively. ρ the mass density of target, and $Q(t)$ is the heat generated in the target by both the green and IR laser irradiation, and is defined as

$$Q(t) = (1 - R_{\rm g})\,\alpha_{\rm g}\,I_{\rm g}(t) + (1 - R_{\rm ir})\,\alpha_{\rm ir}\,I_{ir}(t), \qquad (2)$$

where R and α are the reflectivity of the surface and the absorption coefficient, respectively. $I(t)$ the power of laser and subscripts of g and ir indicate green and Infrared laser, respectively. The thermal properties are dependent on temperature, and are obtained from literature[3],

$$k(T) = 0.235 + 4.45\,e^{-T(K)/247} \qquad (3)$$

$$c_{\rm p} = 0.81 + 1.3\times10^{-4}\,T - 1.26\times10^{4}\,T^{-2} \qquad (4)$$

It should be noted that treatment of latent heat of fusion, $L_{\rm f}$, was included in the simulation. The Dirac function $\delta(t$ -

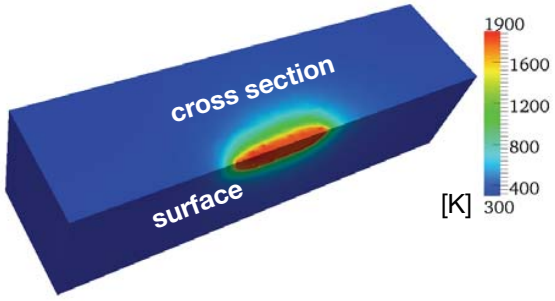

Fig. 5. Thermal distribution simulated by using FreeFEM3D. Three dimensional thermal distribution is shown in cross section.

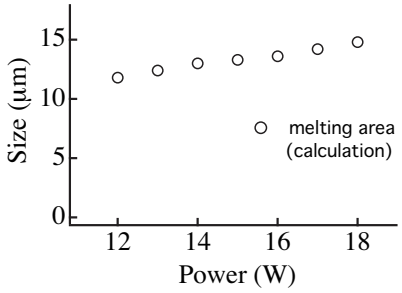

Fig. 6. Melt area on laser annealing. The freeFEM3D shows dependency of the size of melt area on energy fluency of green laser while the NIR laser keep the same energy fluency.

$T_{\rm m}$) is replaced by Gaussian function as

$$\frac{1}{\sqrt{\pi}\,\delta T} exp\left(\frac{-(T-T_{\rm m})^{0.5}}{\delta T^{0.5}}\right), \qquad (5)$$

where $T_{\rm m}$ is the melting temperature and δT, fusion range, was taken to be 30 K. Details of solving the heat transport equation can be found elsewhere [4], [5], [6]. Figure 5 shows three dimensional thermal distribution as an example.

By using freeFEM3D, melt area by laser annealing was evaluated with different energy fluency of green laser. Figure 6 shows dependency of the size of melt area on energy fluency of green laser while the NIR laser keep the same energy fluency. As result, only the NIR laser can not melt the surface; the surface of silicon did not melt with less than the green laser of 4 W even with the NIR laser irradiation. In the range of power between 12 and 18 W, in which the silicon surface re-crystallized experimentally, the melt area shows relatively constant size between 6.5 and 7.5 μm.

IV. Summary

As application of re-activation of backside on power device Insulated Gate Bipolar Transistor (IGBT), laser annealing was employed to irradiate amorphous silicon substrate. Resistivities measured using four point probe showed asymmetric resistance, however, scanning speed of 300 m/min. together with the assist of NIR laser. The thermal simulation was employed to estimate surface temperature, showing the size of melt area stabilized around 7 μm with the laser power between 12 and 18 W.

Acknowledgment

The authors would like to thank Yoshitsugu Sato at Kanagawa Industrial Technology Center for technical support. This research was supported in part by Grants-in-Aid for Scientific Research, Japan Society for the Promotion of Science.

References

[1] J. P. Biersack and L. Haggmark, "Srim - the stopping and range of ions in matter," *Nucl. Instr. and Meth.*, vol. 174, p. 257, 1980.
[2] J. F. Ziegler, J. P. Biersack, and M. D. Ziegler, *SRIM: The Stopping and Range of Ions in Matter*. 860 Aviation Parkway; Suite 300; Morrisville, NC, 27560 USA: Lulu Press Co., 2008.
[3] S. de Unamuno and E. Fogarassy, "A thermal description of the melting of c- and a-silicon under pulsed excimer lasers," *Appl. Surf. Sci.*, vol. 36, pp. 1 – 11, 1989.
[4] R. F. Wood and G. E. Giles, "Macroscopic theory of pulsed-laser annealing. i. thermal transport and melting," *Phys. Rev. B*, vol. 23, no. 6, p. 2923, 1981.
[5] K. Shimizu, S. Imai, O. Sugihara, and M. Matsumura, "Transient temperature profiles in silicon films during pulsed laser annealing," *Jpn. J. Appl. Phys.*, vol. 30, no. 11A, pp. 2664–2672, 1991.
[6] J. R. Kohler, R. Dassow, and J. Werner, "Numerical modeling of high repetition rate pulsed laser crystallization of silicon films on glass," *Mat. Res. Soc. Sympo. Proc.*, vol. 685E, pp. D10.3.1–D10.3.6, 2001.